JTTEE5 2:345-350

Entrainment and Demixing in Subsonic Argon/Helium Thermal Plasma Jets

J.R. Fincke, W.D. Swank, and D.C. Haggard

The velocity, temperature, entrained air fraction, and Ar/He concentration profiles were measured in a subsonic thermal plasma jet using an enthalpy probe and mass spectrometer. Through interaction with the surrounding atmosphere, air is quickly entrained into the jet, resulting in rapidly decreasing velocities and temperatures. Due to the difference in ionization potential, a significant diffusive separation or demixing of Ar and He is also observed in the large temperature gradients present. Near the exit of the torch, in the jet center, the relative He concentration is enhanced by approximately 50% over that of the premixed feed gases. Demixing occurs primarily in the discharge region and torch nozzle. As jet mixing progresses in the downstream direction, the Ar to He ratio approaches the initial input ratio.

1. Introduction

THE entrainment of cold gas into turbulent, high-temperature, and high-velocity atmospheric pressure plasma jets dominates their behavior.[1] Entrainment alters chemical composition and greatly influences velocity and temperature profiles. Ultimately, heat and momentum transfer to injected particles is affected. In addition, the presence of oxygen in the plasma spraying of reactive particles can result in the formation of oxides, generally degrading the coatings produced. The entrainment process has been the subject of several recent investigations.[2-5] The evidence suggests that entrainment is more of an engulfment process[1-4] rather than simple diffusion. The cold engulfed gas bubbles are rapidly transported toward the core of the jet by turbulence, quickly cooling and slowing the jet. These entrained lumps of fluid are subsequently broken down into smaller and smaller scales. During this process, the interfacial area rapidly increases. Once the interfacial zones start to overlap, molecular diffusion quickly annihilates the local concentration gradients and homogenizes the mixed fluid. Dissipation of these bubbles is a relatively slow process, and they persist well downstream. The result is an effective lowering of the average temperature experienced by entrained particles.

The entrainment and mixing characteristics of jets are primarily dependent on the nozzle exit diameter, jet Mach number, and density ratio of the flow field. The velocity and temperature profiles at the nozzle exit play an important, but generally secondary, role. The density ratio is defined as the density of the surroundings into which the jet issues divided by the density of the jet itself. For high-temperature plasma jets, this ratio approaches 70. The Mach number characterizes the effects of compressibility on the dynamics of the jet. Mach numbers for plasma jets vary from 0.5 for typical subsonic guns up to 2 or more for some supersonic guns. In general, high density ratio jets decay faster than low density ratio jets, whereas higher Mach number jets typically exhibit the opposite trend.

In addition to entrainment, the composition of the plasma can be altered by demixing of the plasma gases. Inside the torch, very large temperature gradients and concentration gradients of both the neutral and charged particles exist. This results in thermal diffusion, normal mass diffusion, and ambipolar diffusion. Because diffusion rates depend on the characteristics of the constituents (mass, viscosity, ionization potential, etc.), the result is diffusive demixing of the gaseous species. The effect is well known in both high-pressure and low-pressure stationary discharges.[6-13] Near the torch exit, Ar depletion in the core of Ar/He thermal plasma jets due to ambipolar diffusion in the discharge region is observed. These demixing effects persist for some distance downstream and are slowly remediated by jet turbulence.

In this article, measurements of entrainment and demixing effects were obtained by enthalpy probe measurement. Originally developed in the 1960s, enthalpy probes[14-19] currently are enjoying renewed application to a number of thermal plasma processing problems.[20-24] Their range of application has been extended by integration with a mass spectrometer for measurement of gas composition,[24] and their performance has been validated over a wide range of Mach numbers by comparison to laser scattering measurements.[25,26] Results show rapid entrainment of external air and significant demixing of the Ar and He plasma gas.

2. Enthalpy Probe

The enthalpy probe, its operation, and performance have been described elsewhere.[24,25] The probe itself is copper, has an outside diameter of 4.8 mm, and is integrated with a mass spectrometer for measurement of gas composition. The quadrapole mass spectrometer or residual gas analyzer (RGA) (Leybold-Heraeus Inficon Quadrex 100) samples the gas drawn through the probe. The RGA is set up in a differentially pumped vacuum system. The sample line for the RGA is evacuated with a roughing pump to a pressure of approximately 1 torr. This pressure is regulated with a controlled leak at the probe and is low enough to provide good response time but high enough to prevent preferential pumping of different sized molecules. A sec-

Key Words: argon/helium plasmas, diagnostics, enthalpy probe, entrainment control, mass spectrometer, plasma jet

J.R. Fincke, W.D. Swank, and **D.C. Haggard,** Idaho National Engineering Laboratory, E G & G Idaho, Inc., P.O. Box 1625, Idaho Falls, Idaho 83415.

ond controlled leak is located very close to the quadrapole sensor and is adjusted to maintain the pressure in the sensor vacuum system at approximately 10^{-6} torr. Data acquisition, sample sequencing, and probe positioning, via a three-axis translation stage, are completely computer controlled.

The difficulty in the use of intrusive enthalpy probe techniques in common thermal plasma jets, where large radial gradients exist, is the distortion in the measured velocity and temperature profiles due to streamline displacement. That is, the stagnation or sampled streamline does not originate on the axis of the enthalpy probe. The streamline displacement is always toward the low-velocity side of the jet; hence, the probe measures a streamline that originated in a higher velocity, higher temperature region. Based on an approximate, inviscid, incompressible, and isothermal analysis,[27-29] it has been shown that the nondimensional streamline displacement, δ/D, where D is the probe diameter, is a function of the nondimensional radial velocity gradient, $(D/2U) \cdot (dU/dr)$. For profiles that are approximately Gaussian in shape, the nondimensional radial velocity gradient increases approximately linearly with increasing radius. Hence, the largest streamline displacements are found in the periphery of the jet. Near the jet centerline, the displacement error is small, and probe performance in both subsonic and supersonic compressible flows compares remarkably well with laser scattering results.[25,26] As the jet spreads and the radial velocity gradients decrease, the effect of streamline distortion also decreases. In spite of the drawbacks, enthalpy probes will continue to find wide application in thermal plasma research, due to their relatively low cost and ease of use. Within the limitations noted, high-quality velocity, temperature, and composition data can be produced over a wide range of conditions.

3. Measurement Uncertainty

The 2σ uncertainty in measured enthalpy is estimated to be 5.3%, with the major source of error being the determination of the gas mass flow rate through the probe. This error stems primarily from the inaccuracy of the thermocouple temperature measurement upstream of the sonic orifice. At high temperatures (above 6000 K), moderate changes in the enthalpy of the gas mixture produce small changes in the gas temperature. For this reason, the combination of a 5% uncertainty in properties and a 5.3% uncertainty in the measured enthalpy results in an acceptable 2σ uncertainty of 4.9% in temperature. The 2σ uncertainty on velocity is 6.3%, and its major source of error is uncertainty in the density of the gas mixture. Combining the individual uncertainties on the density, velocity, and enthalpy yields an overall 2σ uncertainty on the integrated energy of 14.9%, which is in good agreement with the values obtained in performing an overall energy balance.[24]

The limitations of the mass spectrometer and the largest source of error reside in the resolution of its 8-bit digitizer. For example, when measuring low concentrations of argon in air, say 10%, the amplitude of the argon mass signal is 5 out of a possible 25, and a single bit error in this signal results in 20% uncertainty. Thus, a signal that oscillates from a value of 5 to 6 is only known within 20% of reading. This resolution error is minimized by optimizing the operating voltage of the electron multiplier and by adjusting the individual mass channel electronic gains until a reasonable sensitivity is achieved. Optimizing the gain in this manner results in an uncertainty of 10% in the air fraction measurement, when the air fraction is in the neighborhood of 0.2. The uncertainty in the Ar/He ratio is also estimated to be 10%.

4. Results and Discussion

The plasma torch (Miller SG-100, Miller Thermal, Inc., Appleton, WI) was operated with a standard anode and cathode combination (Miller No. 165 and 129, respectively). The torch had an 8-mm nozzle exit diameter and was operated at subsonic conditions. Torch operating conditions for the data presented are 900 A at 35 V, for a total power input of 31.5 kW. Approximately 67% of the input power is deposited in the torch gas. The argon and helium flow rates, including powder gas flow, were 3200 L and 1331 L/h, respectively, resulting in an Ar/He mixture ratio of 2.4. The atmospheric pressure was 85.5 kPa.

4.1 *Flow Field*

Radial scans were made from –20 to +20 mm at regular intervals on the longitudinal axis of the torch between 5 and 90 mm. The torch centerline is at 0 mm. The centerline decay of velocity and temperature are shown in Fig. 1 and 2. The sharp decrease in velocity and temperature corresponds to the steep increase of entrained air fraction (Fig. 3). There is a noticeable change in the slope in both the velocity and temperature curves at approximately 15 mm, corresponding to the point at which the mixing layer reaches the jet centerline and the concentration of air in the core region becomes significant. The entrainment and mixing process is more or less complete at 50 mm, also corresponding to a noticeable change in slope in the velocity and temperature curves. At this point, the mixing process has flattened the radial gradients and spread the flow field (Fig. 4) to the point that the rate of decay in velocity and temperature is greatly decreased. The centerline argon/helium ratio (Fig. 5) is approximately 1.6 at the 5-mm axial location. Between 5 and 20 mm, the ratio continues to decrease due to diffusive demixing. At 20 mm, the

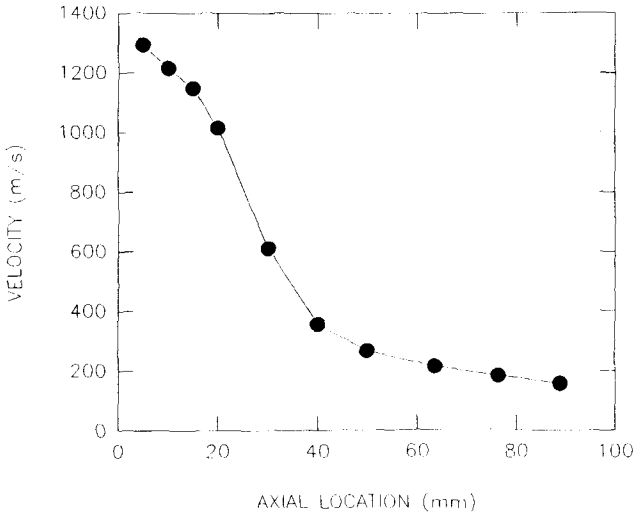

Fig. 1 Plot of centerline axial velocity versus axial location.

shear layer surrounding the jet has reached the centerline. At this point, turbulent mixing overcomes diffusive demixing, and the Ar/He ratio starts to increase.

The decay of centerline velocity and temperature in jets is a function of density ratio and Mach number or compressibility.[30] The density ratio is defined as the ratio of the surrounding density, ρ_e, to jet centerline density, ρ_j. Higher density ratio jets decay faster than lower density ratio jets and compressibility effects tend to inhibit mixing and decay. Using a correlation from Ref 31 for centerline velocity decay of jets without ionization (non-plasma), the effects of density ratio and Mach number (compressibility) can be compared (Fig. 6). From the plot, it can be seen that cold jets, with unity density ratio, decay more slowly than large density ratio jets, and all other things being equal, increasing the Mach number will tend to inhibit decay. Also shown are the measured data from this study, plotted on nondimensional coordinates. Although the agreement is not perfect, the trend is reasonably well represented.

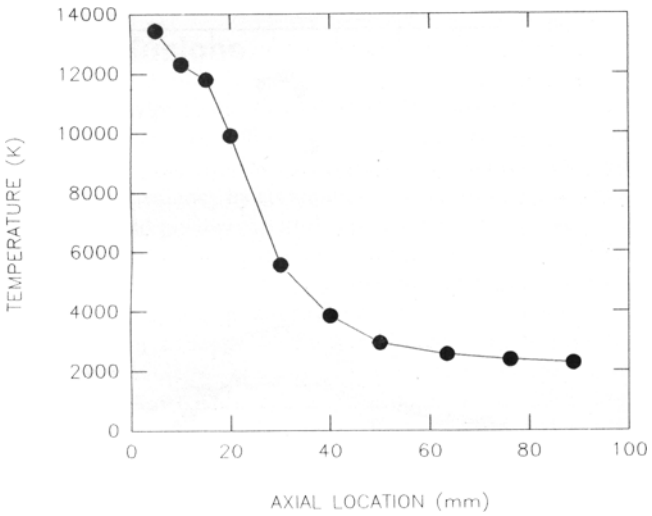

Fig. 2 Plot of centerline temperature versus axial location.

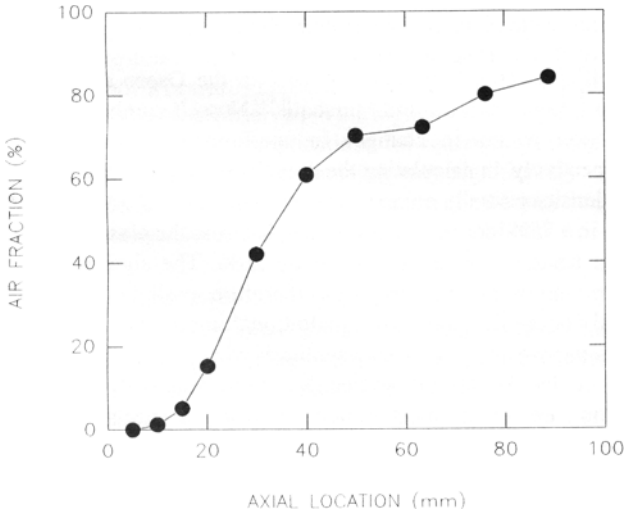

Fig. 3 Plot of centerline entrained air fraction versus axial location.

Plots of velocity and temperature versus radial position at various axial locations appear in Fig. 7 and 8, respectively. In the periphery of the jet, near the torch exit, the gradients of velocity and temperature are very steep. This corresponds with the radial profiles of entrained air fraction (Fig. 9). As the external atmosphere is entrained, the jet slows and spreads and the profiles flatten. The gas is predominately air at typical substrate locations (63.5 to 88.9 mm). A plot of Ar/He ratio versus radial position is shown in Fig. 10 for axial locations of 20 mm (minimum centerline Ar/He ratio) and 50 mm, i.e., the point at which the rate of mixing decreases noticeably. At the center of the jet, the amount of argon relative to helium is 1.4 compared to a ratio of 2.4 for the premixed plasma gas. In the periphery of the jet, the ratio is 2.6, slightly elevated over the premixed value. At 50 mm, the Ar/He profile has been flattened by the mixing process and is approaching the initial ratio of 2.4 in the jet fringes. For radial locations greater than ±10 mm, the Ar and He concentration is so low that measurements are not reliable.

4.2 *Demixing*

The observed enhancement in helium concentration over that of the premixed feed gases by almost a factor of two near the torch exit was driven by diffusive demixing in the discharge region. Due to the differences in ionization potential for argon (15.8 eV) and helium (24.6 eV), a significant number of argon atoms and relatively few helium atoms were ionized, resulting in ambipolar diffusive separation, or demixing, in the presence of large temperature gradients. In addition to ambipolar diffusion, when two particles (an electron and ion) are created by the ionization of argon, the molar concentration of the helium is de-

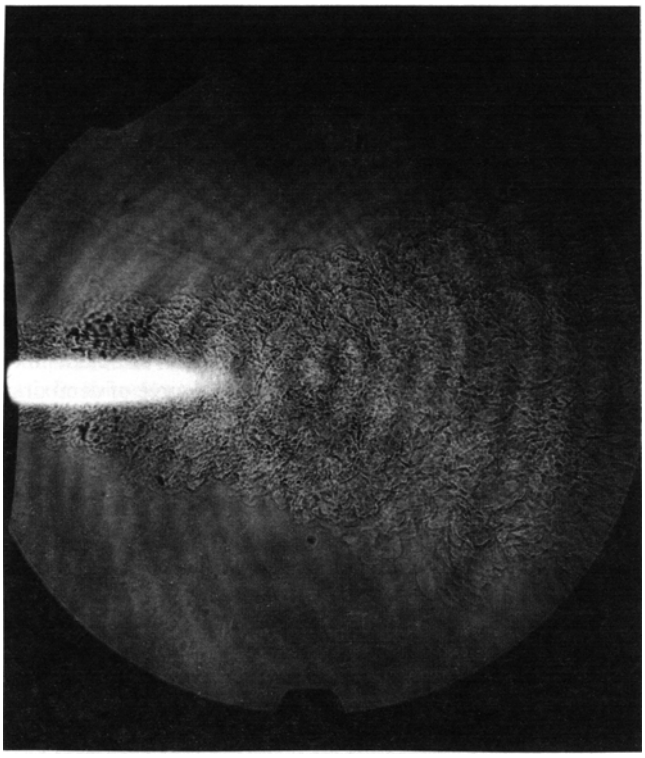

Fig. 4 Pulsed Schlieren or plasma flow field. For reference, the circular image is 75 mm in diameter.

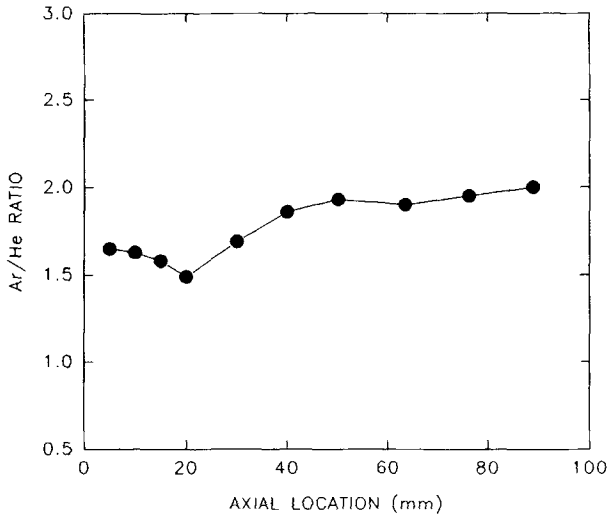

Fig. 5 Plot of centerline argon/helium ratio versus axial location.

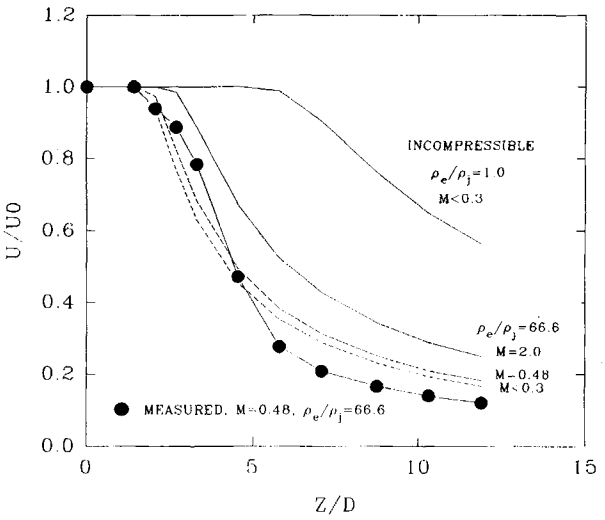

Fig. 6 Comparison of density and Mach number effects.

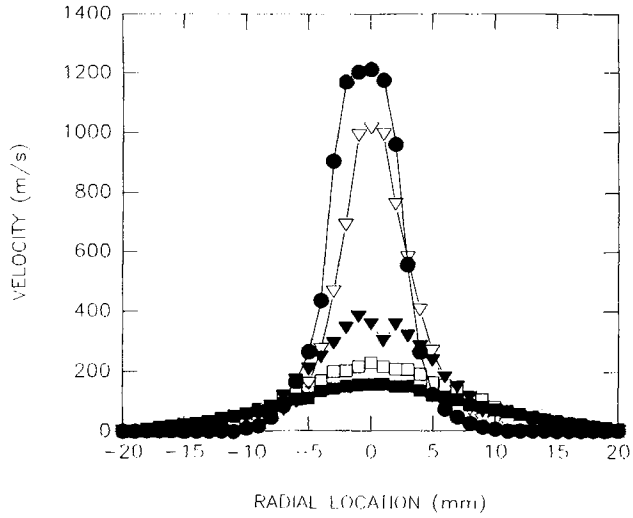

Fig. 7 Plot of axial velocity versus radial location. λ 10 mm. ∇ 20 mm. τ 40 mm. o 63.5 mm. v 88.9 mm.

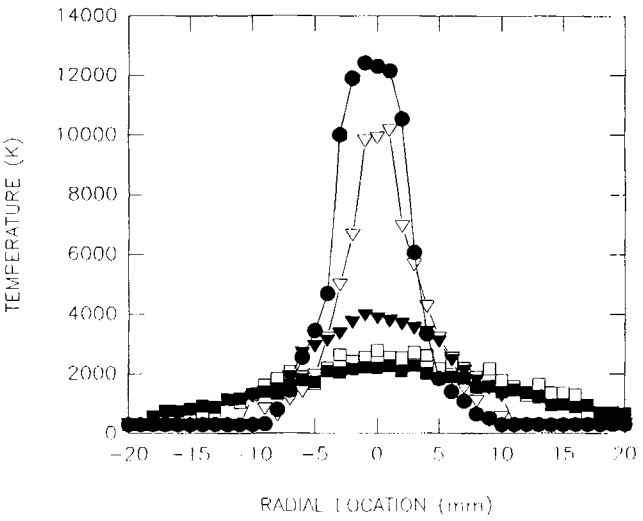

Fig. 8 Plot of temperature versus radial location. λ 10 mm. ∇ 20 mm. τ 40 mm. o 63.5 mm. v 88.9 mm.

creased. This resulted in a helium atom concentration gradient, which tends to diffuse helium toward the jet core. The process continues in the jet core, near the torch exit, until turbulent mixing overwhelms the diffusion process. The degree of demixing was determined primarily in the discharge.

The enhancement of He concentration on the jet centerline, near the nozzle exit, results in an increase in gas viscosity (at 12000 K) of ~15% and an increase in thermal conductivity on the order of 30% over that of the input mix. At the same time, the density and electrical conductivity are decreased by 15 and 6%, respectively, and the enthalpy is changed by only a few percent. The migration of Ar to the jet fringes increases the nozzle exit boundary layer Reynolds number by ~30%, thus influencing the turbulent characteristics of the exit flow and subsequently the jet dynamics. Demixing also affects the plasma/particle interaction. For a given particle size, the result is a decrease in the particle Reynolds number, based on the difference between plasma and particle velocity, of approximately 25%. Assuming a drag coefficient (C_D) correlation based on the Oseen approximation[32] and the Ranz and Marshall[33] Nusselt number (N_u) correlation results in changes in coefficients of 25 and 5%, respectively. In calculating the drag force from C_D, the changes in density partially compensate for coefficient changes, resulting in a 15% increase in drag force, whereas the plasma/particle heat transfer can be enhanced by 20%. The significance of demixing on plasma spraying is therefore small, but not necessarily negligible. There is an additional implication in reactive plasma spraying and plasma synthesis where other gases, generally molecular, are introduced. Due to the relatively low dissociation energy of most molecular gases, a similar diffusive separation can take place. The molecules are predominately dissociated in the high-temperature regions of the plasma, resulting in large concentration gradients that drive the diffusion of the constituent atoms.

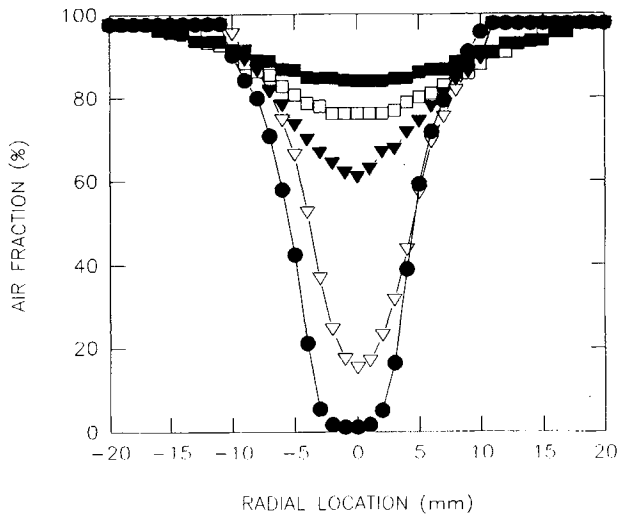

Fig. 9 Plot of entrained air fraction versus radial location. λ 10 mm. ∇ 20 mm. τ 40 mm. o 63.5 mm. v 88.9 mm.

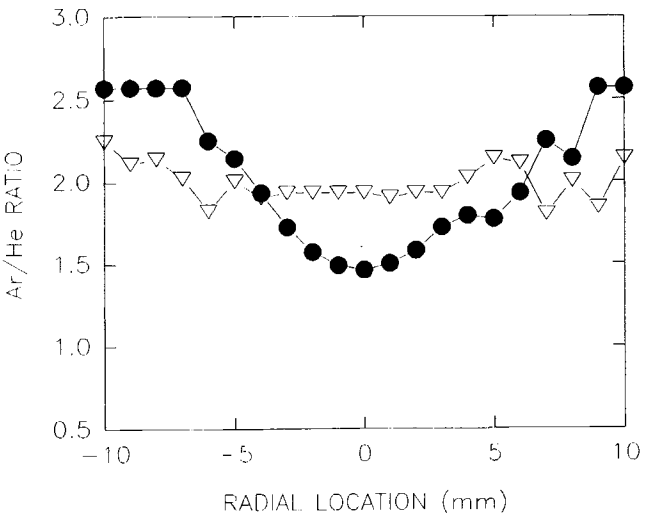

Fig. 10 Plot of argon/helium ratio versus radial location. λ 20 mm. ∇ 50 mm.

5. Conclusions

The enthalpy probe is a robust tool for studying thermal plasmas. Complete maps of the gas flow field including velocity, temperature, and species concentration are made with relative ease and expediency by automation of both data acquisition and sequence and position control. The enthalpy, temperature, and velocity obtained all depend on accurate calculation of the thermodynamic properties of the gas mixture. Accurate properties in turn depend on accurate measurement of the gas composition. Incorporating a mass spectrometer with the enthalpy probe system has provided a quantitative measurement of the gas constituents. This yields valuable information on entrainment, demixing, diffusion, and chemical reactions taking place in thermal plasmas.

The rapid entrainment of air into thermal plasma jets quickly cools and slows the jet. The dynamics of the process are dominated by the large density ratio of thermal plasma jets, with compressibility or Mach number effects playing a secondary role. At typical substrate locations, the gas is predominately air. The ratio of argon to helium at the torch exit is altered in the discharge by diffusive demixing. The effect on jet and particle behavior is small, but not necessarily negligible. Although little demixing of the entrained air was observed in the highly turbulent jet studied here, there may still be implications for reactive spraying and plasma synthesis. Diffusive demixing may significantly affect the concentrations of injected reactive gases and may impose limits on reaction rates and degree of reaction attained.

Acknowledgments

This work was supported by the U.S. Department of Energy, Assistant Secretary for Energy, Office of Basic Energy Sciences under DOE contract No. DE-ACO7-76ID01570.

References

1. E. Pfender, J.R. Fincke, and R. Spores, Entrainment of Cold Gas into Thermal Plasma Jets, *Plasma Chem. Plasma Proc.*, Vol 11, 1991, p 529-542
2. J.R. Fincke, R. Rodriguez, and C.G. Pentecost, Coherent Anti-Stokes Raman Spectroscopic Measurement of Air Entrainment in Argon Plasma Jets, *Plasma Processing and Synthesis of Materials III*, Materials Research Society Symposia Proc., Vol 190, D. Apelian and J. Szekely, Ed., 1991, p 184-189
3. J.R. Fincke, R. Rodriguez, and C.G. Pentecost, Measurement of Air Entrainment in Plasma Jets, *Thermal Spray Research and Applications*, T.F. Bernecki, Ed., ASM International, 1991, p 45-48
4. R. Spores and E. Pfender, Flow Structure of a Turbulent Plasma Jet, *Thermal Spray: Advances in Coatings Technology*, D.L. Houck, Ed., ASM International, 1988, p 85-92
5. M. Vardelle, A. Vardelle, Ph. Roumilhac, and P. Fauchais, Influence of the Surrounding atmosphere Under Plasma Spraying Conditions, *Thermal Spray: Advances in Coatings Technology*, D.L. Houck, Ed., ASM International, 1988, p 117-121
6. W. Frie and H. Maecker, Massentrennung durch Diffusion Reagierender Gase, *Z. Physik Bd.*, Vol 162, 1961, p 69-83 (in German)
7. H. Maecker, Fortschritte in der Bogenphysik, *Proc. 5th Int. Conf. Ionization Phenomena in Gases*, North-Holland, p 1793-1811
8. J. Richter, Uber Diffusionsvorgange in Lichtbogen, *Z. Astrophysik*, Vol 53, 1961, p 262-272 (in German)
9. W. Frie, Berechnung der Gasusammensetzung und der Materialfunktionen von SF_6, *Z. Physik, Bd.*, Vol 201, 1967, p 269-294, in German
10. D. Vukanovic and V. Vukanovic, On the Behavior of Hydrogen Isotopes in a DC Arc Plasma, *Spectrochimica Acta*, Vol 24B, 1969, p 579-583
11. G. Baruschka and E. Schulz-Gulde, Transition Probabilities for F I Lines from Wall Stabilized Arc Measurements, *Astronotics Astrophysics*, Vol 44, 1975, p 335-342
12. E. Fisher, Axial Segregation of Additives in Mercury-Metal-Halide Arcs, *J. Appl. Phys.*, Vol 47, 1976, p 2954-2960
13. H.-P. Stormberg, Axial and Radial Segregation in Metal Halide Arcs, *J. Appl. Phys.*, Vol 52, 1981, p 3233-3237
14. J. Grey, Thermodynamic Methods of High-Temperature Measurement, *ISA Trans.*, Vol 4, 1965, p 102-115
15. S. Katta, J.A. Lewis, and W.H. Galvin, A Plasma Calorimetric Probe, *Rev. Sci. Instr.*, Vol 44, 1975, p 1519-1523
16. J. Grey, P.F. Jacobs, and M.P. Sherman, Calorimetric Probe for the Measurement of Extremely High Temperatures, *Rev. Sci. Instr.*, Vol 33, 1962, p 738-741
17. J. Grey, Sensitivity Analysis for The Calorimetric Probe, *Rev. Sci. Instr.*, Vol 34, 1963, p 857-859

18. T.J. O'Connor, E.H. Comfort, and L.A. Cass, Turbulent Mixing of an Axisymmetric Jet of Partially Dissociated Nitrogen with Ambient Air, *AIAA J.*, Vol 4, 1966, p 2026-2032
19. L.A. Anderson and R.E. Sheldahl, Experiments With Two Flow-Swallowing Enthalpy Probes in High-Energy Supersonic Streams, *AIAA J.*, Vol 9, 1971, p 1804-1810
20. W.L.T. Chen, J. Heberlein, and E. Pfender, "Experimental Measurements of Plasma Properties for Miller SG-100 Torch with Mach I Settings. Part 1: Enthalpy Probe Measurements," Report, Engineering Research Center for Plasma-Aided Manufacturing, Dept. of Mech. Engr., Univ. of Minn., Aug 1990
21. M. Brossa and E. Pfender, Probe Measurements in Thermal Plasma Jets, *Plasma Chem. Plasma Proc.*, Vol 8, 1988, p 75-90
22. A. Capetti and E. Pfender, Probe Measurements in Argon Plasma Jets Operated in Ambient Argon, *Plasma Chem. Plasma Proc.*, Vol 9, 1989, p 329-339
23. P. Stefanovic, P. Pavlovic, and M. Jankovic, High Sensitive Calorimetric Probe for Diagnostics Thermal Plasma at the Exit of Electric Arc Heater, *Proc. 9th Int. Symp. Plasma Chemistry*, IUPAC, Vol 1, 1989, p 314-319
24. W.D. Swank, J.R. Fincke, and D.C. Haggard, Modular Enthalpy Probe and Gas Analyzer for Thermal Plasma Measurements, *Rev. Sci. Instr.*, Vol 64, 1993, p 56-62
25. J.R. Fincke, S.C. Snyder, and W.D. Swank, Comparison of Enthalpy Probe and Laser Light Scattering Measurement of Thermal Plasma Temperatures and Velocities, *Rev. Sci. Instr.*, Vol 64, 1993, p 711-724
26. J.R. Fincke, W.D. Swank, S.C. Snyder, and D.C. Haggard, Detached Shock Enthalpy Probe Performance, *Proc. Int. Symp. Plasma Chemistry*, ISPC-11, IUPAC, Leicestershire, UK, Aug 1993, p 475-480
27. I.M. Hall, The Displacement Effect of a Sphere in a Two-Dimensional Shear Flow, *J. Fluid Mechan.*, Vol 1, 1956, p 142-162
28. M.J. Lighthill, Contributions to the Theory of the Pitot-Tube Displacement Effect, *J. Fluid Mechan.*, Vol 2, 1957, p 493-512
29. P.O.A.L. Davies, The Behavior of a Pitot Tube in Transverse Shear, *J. Fluid Mechan.*, Vol 3, 1957, p 441-456
30. G.L. Brown and A. Roshko, On Density Effects and Large Structure in Turbulent Mixing Layers, *J. Fluid Mechan.*, Vol 64, 1974, p 775-816
31. P.O. Witze, Centerline Decay of Compressible Free Jets, *AIAA J.*, Vol 12, 1974, p 417-418
32. H. Schlichting, *Boundary Layer Theory*, McGraw Hill, 1968, p 17
33. W.E. Ranz and W.R. Marshall, Jr., *Chem. Eng. Prog.*, Vol 48, 1952, p 141 and Vol 48, 1952, p 173